Crack Linkup by Stable Crack Growth

L. Ma [1], A.S. Kobayashi[2], S. N. Atluri[3], P.W. Tan[4]

Abstract: Experimentally determined T_ε^* and CTOA resistance curves were used to simulate numerically, stable crack growth and the ensuing crack linkup in 0.8 *mm* thick 2024-T3 aluminum tension specimen with multiple site damage (MSD) subjected to monotonically/cyclically increasing loading. The T_ε^* integral correctly predicted the crack growth and linkup history as well as the onset of rapid fracture in MSD specimens. The CTOA criterion also predicted the crack growth history but in its present form, could not predict crack linkup and rapid fracture.

keyword: stable crack growth, crack linkup, T_ε^* integral, CTOA, multiple site damage (MSD)

1 Introduction

Crack initiation at multiple sites in a riveted structure is governed by the local conditions, such as the rivet load, the frictional load, rivet clamp-up, secondary bending, and the initial residual stress [Schijve (1995)]. Successive coalescence of these in-line short cracks could form a long lead crack which could then grow to a critical length. Thus the failure scenario of MSD initiates with a long lead crack which is surrounded by many smaller cracks where the interaction of these crack reduces the residual strength of the structure.

Gruber, Wilkins and Worden (1996) used linear elastic fracture mechanics (LEFM) to predict the MSD crack linkup and the fracture load for several stiffened panels. When compared with test results, their LEFM analysis over predicted the crack linkup stress but under predicted the linkup load when an Irwin plastic zone adjustment was made. DeWit, Fields, Mordfin, Low and Harne (1994) also found that LEFM over predicted the crack linkup stress by 20% and under predicted the final fracture stress by as much as 15%. Nathan and Brot (1991) developed an analytical stress intensity factor solution by combining the individual geometry effects of equal and unequal sized cracks as well as for loaded and unloaded fastener holes. Their calculated stress intensity factor compared well with finite element (FE) analysis and the test results. However, the J integral obtained via LEFM, i.e. $J = G = K^2/E$, differed substantially with the elastic-plastic J integral. For MSD cracks of 3.2 *mm*, $J_{elastic}$ was 15% less than $J_{elastic\text{-}plastic}$ [Nathan and Brot (1995)].

Swift (1985, 1992, 1994) postulated a link up of two cracks when the ligament material reached the yield stress. This criterion was based on the observation that full, plane-stress fracture toughness could not be achieved unless the panel width is greater than 1270 *mm* (50 inches). Panels less than 1270 *mm* in width failed by net section yielding prior to reaching the critical stress intensity factor. Although a typical fuselage skin panel was greater than 1270 *mm*, Swift assumed that the effective panel width was equal to the fastener pitch of the collinear fastener holes and that the ligament between two adjacent cracks would fail by net section yielding when the two plastic zones, as per Irwin's formula, linked up.

Gruber, Wilkins and Worden (1996) also used the net section yielding method and compared the predicted results with the MSD tests performed at Boeing, NIST, and Foster Miller. Approximately half of the cases analyzed by this method had errors greater than 10%. In some cases, the predicted link-up stress was higher than the failure stress of a panel with a lead crack and no MSD cracks.

More recently, Nishimura (1999) used a strip yield model to estimate the coalescence condition of the plastic zones for multiple cracks in a riveted stiffened sheet. Limited numerical results for this theoretical model were obtained by iteratively solving for critical values of remote stress, fastener forces, plastic zone sizes and crack tip opening displacement.

The above brief review suggests that neither LEFM nor the LEFM based plastic zone can account for the large plastic deformation at the long lead crack tip. The purpose of this study is to establish a methodology based on a newly developed ductile fracture criteria, i.e. the T_ε^* integral and the crack tip opening angle (CTOA), to predict stable crack growth in a ductile material, MSD crack linkup and the residual strength of a structure containing MSD.

2 T_ε^* Integral Criterion

The T_ε^* integral for a stationary crack is identical to the popular J integral which is characterized by the deformation theory of plasticity. However, for a quasi-statically extending crack, where the deformation theory of plasticity is no longer

[1] University of Washington, Department of Mechanical Engineering, Seattle, WA 98195-2600. Currently at United Technologies Research Center, Structural Integrity Group, East Hartford, CT 06108

[2] University of Washington, Department of Mechanical Engineering, Seattle, WA 98195-2600

[3] University of California, Los Angeles, Center for Aerospace Research and Education, Los Angeles, CA, 90095-1597

[4] FAA William J. Hughes Technical Center, Atlantic City International Airport, NJ 08405

valid, T_ε^* and J integrals differ substantially. The T_ε^*-integral [Stonesifer and Atluri (1982); Atluri, Nishioka and Nakagaki (1984)], which is a *near-field* integral based on the incremental theory of plasticity, varies with the near field integration contour and should be evaluated near the crack tip if it is to be considered a crack tip parameter. Once the near field integration contour, Γ_ε, is specified, the general form of the T^* integral [Atluri, Nishoka and Nakagaki (1994)], which incorporates Γ_ε in its integration contour, is path independent regardless of the size of the outer contour. Thus unlike the J integral, the T_ε^* integral is a path independent integral in the presence of large scale yielding and unloading.

For a straight crack which is subjected to a self-similar straight crack propagation,

$$T_\varepsilon^* = \int_{\Gamma_\varepsilon}\int_{\Gamma_\varepsilon} \left[W n_k - s_{ij} n_j u_{j,k}\right] d\Gamma \tag{1}$$

where W is the strain energy density and i, j and $k = 1, 2$. The indices, 1 and 2, represent the Cartesian coordinates parallel and perpendicular to the straight crack. Since the direction normal, $n_1 = 0$, and the stresses, $s_{12} = s_{22} = 0$, the integrand in Eq. 1 vanishes in the trailing wake of the crack when Γ_ε is very close to the traction-free crack. This nearness, ε, is set to the thickness of the specimen in order to guarantee a state of plane stress along the integration contour [Okada, Atluri, Omori and Kobayashi (1999)].

In order to account for the prior history effect, the integration contour for the T_ε^* integral extends together with the extending crack [Okada and Atluri (1999)]. The incremental T_ε^*, i.e. ΔT_ε^*, within a given stationary but elongated integration contour are then summed from the initiation of crack extension to its current crack tip location consistent with the incremental theory of plasticity as shown by Brust, Nishioka, Atluri and Nakagaki (1985). By confining the integration contour, Γ_ε, to the vicinity of a traction-free crack and by using the stress/strain fields generated by the incremental theory of plasticity, Pyo, Okada and Atluri (1995) have shown, through numerical experiments, that T_ε^* can be computed by the current T_ε^* without the need to sum ΔT_ε^* for each incremental crack extension.

Since the contour integration no longer involves the unloaded region, the contour integral ahead of the crack tip can now be evaluated by using the deformation theory of plasticity as this frontal region is dominated by the loading process. Not only is the experimentally impractical procedure of evaluating ΔT_ε^* avoided but T_ε^* can now be determined directly from the measured displacement field surrounding a partial contour near and in front of the crack tip. This is a fortunate approximation since the state of stress based on the incremental theory of plasticity cannot be readily computed from the measured displacement and strain fields in the trailing crack wake region.

3 CTOA Criterion

The critical CTOA criterion assumes that stable crack growth occurs when an angle made by a point on the upper surface of a crack, the crack tip, and a point on the lower surface reaches a critical value. For convenience, a point 1 mm behind the crack tip has been used [Newman, Dawicke, and Bigelow (1992); Omori, Kobayashi, Okada, Atluri and Tan (1998)]. Extensive experimental results from thin aluminum fracture specimens have shown that after an initial transient period, the CTOA remains constant throughout Mode I stable crack growth [Dawicke, Newman and Bigelow (1995)]. Moreover, a two-dimension, elastic-plastic finite element simulation of stable crack growth based on the CTOA criterion correctly predicted the load versus crack opening displacement (COD) relations and the Mode I crack extension histories of the fracture specimens.

4 Method of approach

4.1 MSD specimens

The feasibility of using the T_ε^* integral and the CTOA criteria to predict crack growth and linkup in the presence of MSD was tested through a series of MSD experiments. The experimental procedure consisted of determining the T_ε^* integral experimentally and measuring the crack growth and linkup in MSD2 specimens with two cracks, MSD3 specimens with a center/lead crack approaching two holes with MSD cracks and MSD5 specimens with a center/lead crack and four holes. These specimens were machined from Al 2024-T3 clad aluminum sheet of thickness 0.8 *mm*. The T_ε^* resistance curve of this aluminum sheet was determined through stable crack growth tests of single edge notch (SEN) and center notch (CN) specimens. All cracks were oriented in the L-T direction and special buckling guides were used to prevent the out-of-pane buckling of the fracture specimen from buckling. In addition, the uniaxial stress-strain relation of the Al 2024-T3 sheet was determined for the elastic-plastic finite element analysis. Details of the experimental procedure and results are reported in Ma (1999). Figure 1 shows the MSD3 and MSD5 specimens considered in this study. MSD2 specimen, which is not shown in Figure 1, is 50.8 *mm* wide and is similar to the MSD3 specimen but without the center crack.

4.2 Numerical modeling

The FE model consisted of one half or one quarter of a truncated MSD specimen, depending on the number of plane of symmetry, and of graded finite elements with the smallest element of 0.25 mm distributed along the crack axis. Figure 2 shows a typical finite element (FE) model used in simulating numerically, crack growth in the MSD2 specimen. The finite element (FE) analysis was based on the incremental theory of plasticity using the measured equivalent stress-strain relation and accounted for the unloading effect in the trailing wake of

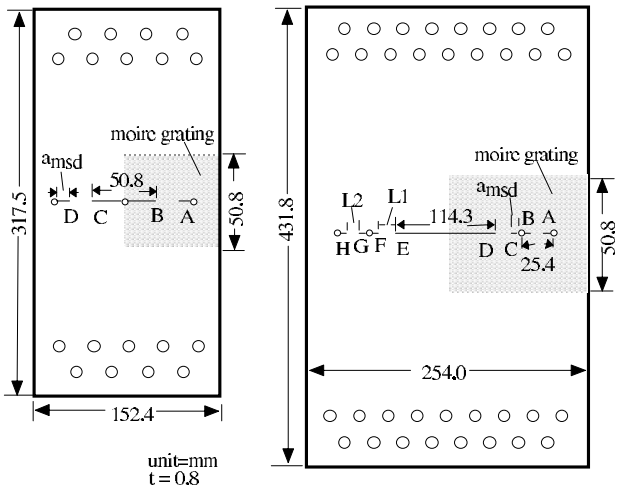

(a) MSD3 (b) MSD5

Figure 1 : MSD3 and MSD5 specimens

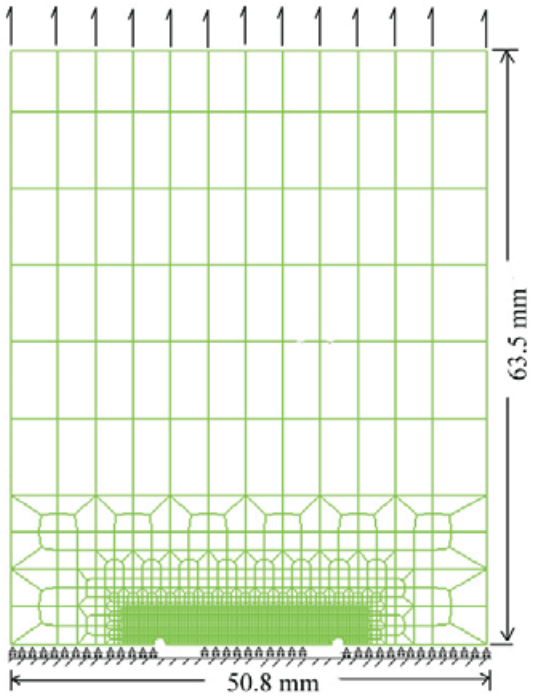

Figure 2 : FE half model of specimen MSD2-05.

the extending crack tip. The T_ε^* integral along an elongated contour surrounding the stably growing crack of the fracture specimens was then computed using the domain integral [Nikishkov and Atluri (1987)] in order to mask the numerical errors in the FE data surrounding the crack tip. Since the COD profile, defined by the nodes behind the tip, is typically jagged such that the crack face could not be easily defined, the slope of the COD profile was used to evaluate the CTOA in this study.

5 Results

5.1 T_ε^* resistance curve

Experimentally determined T_ε^* integral data of one SEN specimen and five CN specimens of different cracks lengths with saw cut or fatigued crack tip are shown in Fig. 3. For a contour size of $\Gamma_\varepsilon = 1$ *mm*, the T_ε^* data for the 152.4 *mm* and 254 *mm* wide specimens are approximately equal. Other than the 50.8 *mm* wide CN specimens, the experimental T_ε^* data of the SEN and CN specimens practically coincide thus suggesting that the T_ε^* is a geometry-independent material property of this material. The T_ε^* resistance curve represents the average of this data.

As shown in Fig. 3, the T_ε^* resistance curve rises at the initial stage of crack growth and reaches a constant value during steady crack growth. In contrast, the global J resistance, J_R, curve continually rises with stable crack extension. This rising J_R includes energy from sources other than the crack tip and thus does not characterize the crack tip. While the J integral based instability criterion is determined on a global basis, the instability criterion for T_ε^* integral is locally based. During steady crack growth, the state of stress is in equilibrium and thus the parameter characterizing this phenomenon should be constant. For T_ε^* the concept of crack extending when the driving force exceed the material's resistance can be applied as $T_\varepsilon^* > T_{\varepsilon R}^*$. However, the concept of $dT_\varepsilon^*/da > dT_{\varepsilon R}^*/da$ cannot be applied since $T_{\varepsilon R}^*$ is constant and $dT_{\varepsilon R}^*/da$ is always zero. Any type of positive $dT_{\varepsilon R}^*/da$ will signify that instability will occur. Thus for T_ε^* integral, only $T_\varepsilon^* > T_{\varepsilon R}^*$ is needed and instability occurs when the T_ε^* remains greater than $T_{\varepsilon R}^*$ without an additional applied load or a displacement.

For crack growth simulation, a load or displacement was applied as the boundary condition and the crack was propagated when $T_\varepsilon^* > T_{\varepsilon R}^*$. With the prescribed load or displacement held constant, T_ε^* was evaluated again for the extended crack. If T_ε^* remained greater than $T_{\varepsilon R}^*$, the crack was extended again, and T_ε^* was re-evaluated. The crack continued to extend until T_ε^* dropped below $T_{\varepsilon R}^*$. Additional load/displacement was applied to the specimen until T_ε^* was equal to $T_{\varepsilon R}^*$ where upon another node was released to extend the crack. This procedure was repeated until no additional load or displacement was required to propagate the crack. At that point, instability was assumed to have occurred.

Crack growth simulations were preformed on nine specimen configurations per the procedure described above. The results were compared with the experimental data to determine how well FE analysis with the T_ε^* integral could predict the crack linkup and failure load. The CN configuration was simulated first to determine if the T_ε^* resistance curve shown in Fig. 3

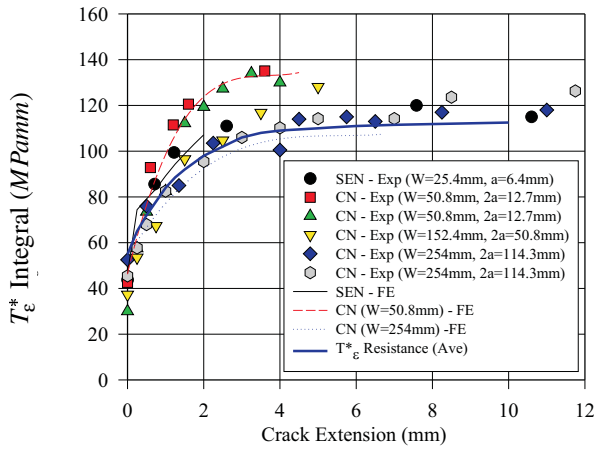

Figure 3 : SEN and CN experimental T_{ε}^{*} resistance curve ($\Gamma_{\varepsilon} = 1\ mm$)

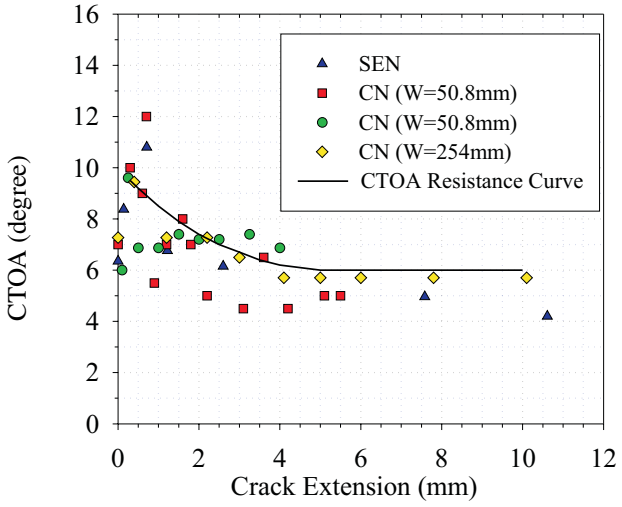

Figure 4 : Experimental CTOA of SEN and CN specimens

could predict crack growth properly.

5.2 CTOA resistance curve

All experimentally determined CTOA had the same profile of being very large and scattered at the initial crack growth ($\Delta a = 1 - 2\ mm$), as shown in Fig. 4, due to crack tunneling and shear lip formation. In the 2-D finite element analysis, the crack tunneling and shear lip formation processes are not modeled and a constant CTOA of 5 to 6 degree is typically used throughout the crack growth process [Newman, Dawicke and Bigelow (1992)]. Such constant CTOA resistance curve would under predict the load in the initial stage of crack growth. An average, which is represented by the curve in Fig. 4, of the experimental data was used as the CTOA resistance curve in this study.

For crack growth simulation in a FE model, the crack was extended when the CTOA reached the critical value of 6 degrees under a prescribed displacement boundary condition. With the displacement held constant, the CTOA was examined again for crack extension. If the CTOA remained greater than 6 degrees, the crack was extended again, and the CTOA was evaluated again. The crack continued to extend until the CTOA dropped below 6 degrees. Additional displacement was applied until the CTOA was greater than 6 degrees where another node was released to extend the crack. This procedure was repeated until no additional displacement was required to propagate the crack. At that point, instability was assumed to have occurred.

6 Simulation studies

6.1 MSD2 specimen

MSD2 specimens contained two equal-length cracks extending toward each other. The hole diameter and the initial fatigue crack length, shown in Fig. 2, were 1.25 *mm* and 4.25 *mm*, respectively. The model consisted of 2438 nodes and 2358 elements with displacement controlled boundary conditions.

The simulated finite element load versus crack extension relation together with the corresponding experimental results are shown in Fig. 5. The predicted maximum load of 10,700 *N* was 6.3% lower than the measured value (11,400 *N*). FE predicted that the maximum load occurred at 0.25 *mm* of crack extension while the experiment showed that the maximum load occurred at 0.5mm of crack extension. FE analysis also predicted crack linkup after 2.0 *mm* of crack extension while the test had only 1 *mm* of stable crack growth. The difference may be attributed to the compliance of the experimental loading system. The FE analysis assumed that the loading frame was perfectly rigid. Despite the fact that a lower $T_{\varepsilon R}^{*}$ curve was use to simulate the crack growth than what was observed for the 50.8 *mm* wide specimen, the residual prediction strength was only 6.3% lower than the test value. Part of this difference could be attributed to the $T_{\varepsilon R}^{*}$ curve, which was 15% higher than the SEN and other CN curves, for the 50.8 *mm* wide CN specimen.

6.2 MSD3 specimen

A quarter FE model of MSD3_08, MSD3_12, and MSD3_13 specimens with the same initial crack lengths and configuration were used in this analysis. The FE model consisted of 2729 nodes and 2625 elements with the smallest elements of 0.25 *mm* by 0.25 *mm*.

The analysis was conducted by displacement controlled boundary conditions and cracks were propagated per the $T_{\varepsilon R}^{*}$ resistance curve. The load vs. crack extension curves for

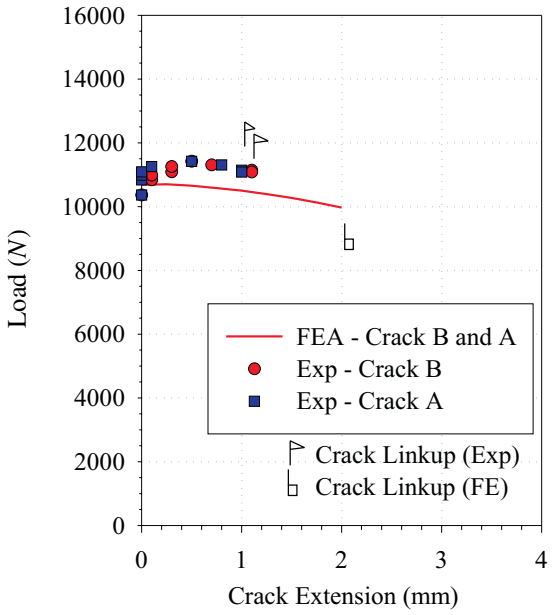

Figure 5 : MSD2_05 reaction load vs. crack growth

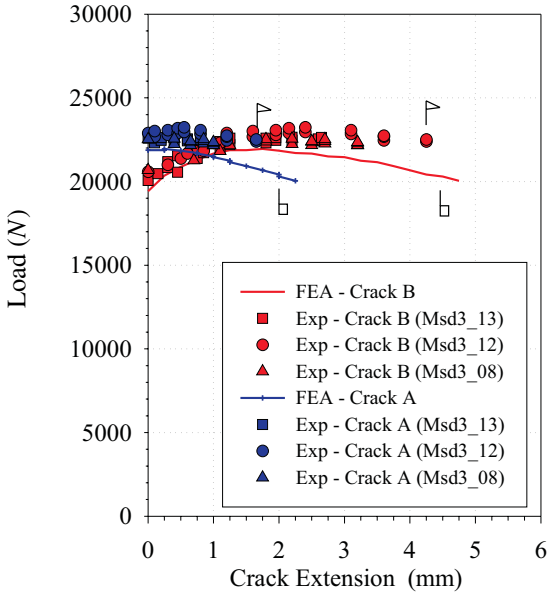

Figure 6 : MSD3_08 reaction load vs. crack growth

MSD3_08 specimen are shown in Fig. 6. Finite element simulation predicted the maximum load of 21,946 N to occur after the center crack extended 1.75 mm. The averaged measured maximum load was 22,813 N after the center crack extended 2.3 mm. The predicted maximum load was 4% lower than the test value. The predicted crack extension at linkup correlated well with the test results. The crack extension results of experiment and FEA were as follows: Δa_{CNFE} of 4.5 mm vs. Δa_{CNtest} of 3.0 – 4.5 mm and Δa_{MSDFE} of 2.0 mm vs. $\Delta a_{MSDtest}$ of 1.0 – 1.6 mm. However, the FE linkup load was 12% lower. Overall, the FE predictions correlated well with test results.

6.3 MSD5 specimen

The FE model consisted of 3876 nodes and 3733 elements with the smallest element of 0.25 by 0.25 mm. Crack growth simulation was performed for specimens MSD5_02, MSD5_05, MSD5_07, MSD5_08, MSD5_11 and MSD5_14. Displacement-controlled boundary conditions were applied in the FE analysis and cracks were propagated per the T_ε^* resistance curve.

MSD5_08 specimen had 2.5 mm MSD cracks and 12.7 mm ligament between the center and first MSD cracks. The specimen failed simultaneously with the first linkup after crack tips D and C extended 2.6 – 2.8 and 0.8 mm, respectively, at a maximum load of 26,535 N. As shown in Fig. 7, FE analysis predicted the maximum load (26,718 N) to occur after the crack tips D and C extended 2.0 and 0.5 mm, respectively, and crack linkup to occur at $a_D = 3.75$ mm and $a_C = 2.0$ mm. FE simulation also predicted that the second linkup to occur at 20,728 N after crack tips B and C extended 3.75 mm and 1.75 mm, respectively. The second linkup load was well below the first maximum linkup load. Thus the predicted maximum load for specimen MSD5_08 was 1% higher than the test value.

Cracks were also propagated with a constant CTOA value of 6 degree. The predicted versus measured reaction load is shown in Fig. 8. The predicted reaction load at the initial stage of crack growth was lower than the test value and the predicted maximum load was 10% lower than the test value. The CTOA criterion, however, did not predict instability. Additional displacement was needed to propagate the crack even though the center crack had extend 7 mm and the MSD crack extended 4 mm with only 1 mm of ligament left between the cracks. The analysis was stopped at that point and the cracks were assumed to have linked. This simulation demonstrated that the CTOA could predict crack growth of ductile material and that it may be used to predict the residual strength of structures containing MSD. However, the prediction at the initial stage of crack growth was approximately 20% lower than the test value when a constant critical CTOA value was assumed. For problems where the structure will fail immediately after crack growth initiation, a constant CTOA value may lead to under predicting of the residual strength.

Overall, the FEA crack growth, crack linkup and residual strength analyses using T_ε^* integral as the fracture criterion correlated very well with experimental data. On the average, the predicted maximum loads differed from test results by only 3.2%. A summary of the results is shown in Table 1.

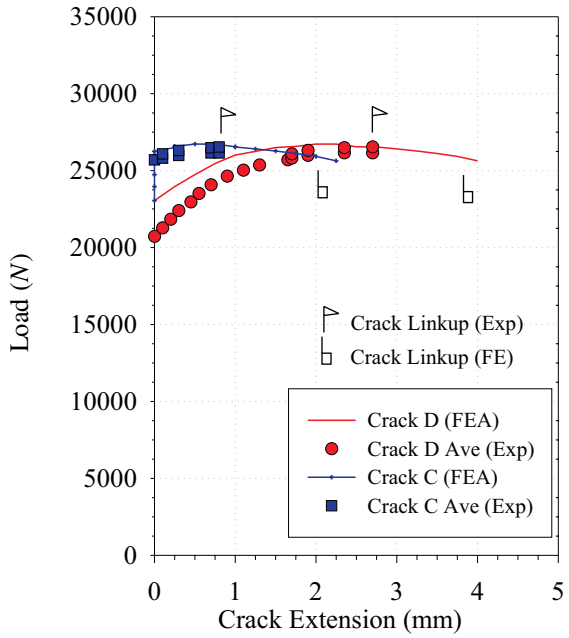

(a) Reaction load of first crack linkup

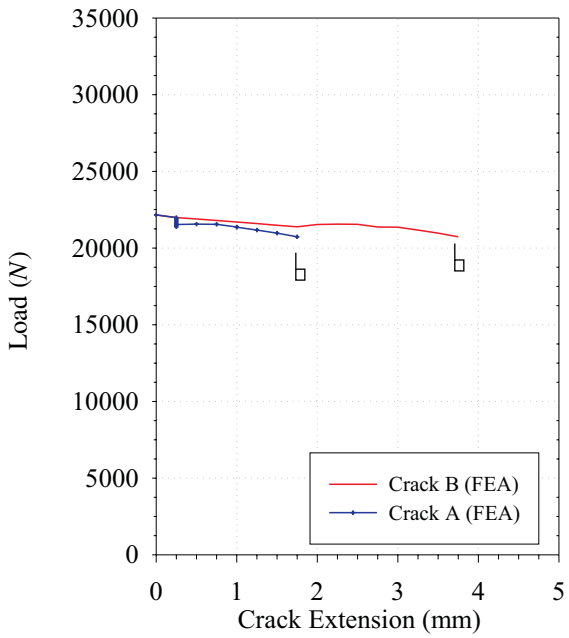

(b) Reaction load of second crack linkup

Figure 7 : MSD5_08 reaction load vs. crack extension

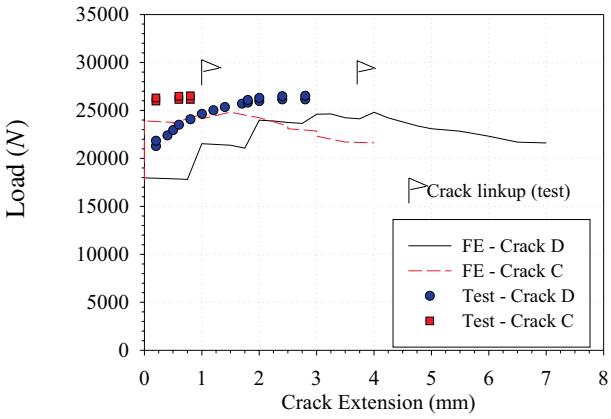

Figure 8 : MSD5_08 reaction load vs. crack growth based on CTOA criterion

7 Discussion

The plastic zone linkup criterion predicts that cracks will link up when the ligament have yielded [Swift (1985)]. In another word, linkup occurs when the plastic zone from two crack tips touched. Swift's derivation used Irwin's plastic zone equation which is one-half of the actual plastic zone size. In this analysis, the following modified Irwin plastic zone equation was used.

$$r_p = \frac{1}{\pi}\left(\frac{K}{\sigma_y}\right)^2 \tag{2}$$

where K is the stress intensity factor and σ_y is the yield stress. K may be expressed as

$$k = \beta\sigma\sqrt{\pi a} \tag{3}$$

where β is the geometric correction factor which accounts for the finite width, the adjacent crack, and the hole effects. The linkup stress may be expressed as

$$\sigma = \sigma_y\sqrt{\frac{L}{a_1\beta_1^2 + a_2\beta_1^2}} \tag{4}$$

The predicted collapse loads based on the plastic zone linkup criterion are shown in Table 2. The yield stress is 310 MPa. Comparisons of the predicted linkup stress to the test results shows that Swift's criterion over predicted the linkup stress by 31% to 78% for the MSD2 and MSD3 specimens and under predicted by as much as 36% for the MSD5 specimens.

Instead of using the yield stress in the above equation, one could argue that yielding does not necessarily lead to failure and the collapse stress $(\sigma_y + \sigma_{ult})/2$ should be used instead.

Table 1 : Crack linkup and residual strength prediction based on the T_ε^* integral criterion.

Specimen	P_{max} of 1^{st} linkup			P_{max} of 2^{nd} linkup			P_{max} of specimen		
	FE (KN)	Test (KN)	% diff	FE (KN)	Test (KN)	% diff	FE (KN)	Test (KN)	% diff
MSD2_05	10.70	11.40	6.3	—	**	**	10.70	11.40	6.3
MSD3_08	21.95	22.81	3.8	—	**	**	21.95	22.81	3.8
MSD5_02	25.45	24.58	3.5	25.24	25.14	0.4	25.45	25.14	1.2
MSD5_05	20.31	19.68	3.2	20.56	18.83	7.5	20.31	19.68	3.2
MSD5_07	28.63	27.32	4.8	22.26	22.34	1.3	28.63	27.32	4.8
MSD5_08	26.72	26.54	0.7	20.73	**	**	26.72	26.54	0.7
MSD5_11	29.12	30.17	3.5	—	**	**	29.12	30.17	3.5
MSD5_14	38.98	38.40	1.5	—	**	**	38.98	38.40	1.5

** Test specimen failed simultaneously with the first linkup.

Table 2 : Crack linkup and residual strength prediction based on the plastic zone linkup criterion prediction

Specimen	$P_{MaxTest}$ (KN)	Predicted P_{Linkup} (KN) ($\sigma_y = 310\,MPa$)	% diff	$P_{MaxTest}$ (KN)	Predicted P_{Linkup} (KN) Assume $\sigma_y = \sigma_{coll} = 379\,MPa$	% diff
MSD2_2	12.24	21.79	+ 78.0	12.24	26.66	+ 117.8
MSD2_7	10.56	15.09	+ 42.9	10.56	18.46	+ 74.8
MSD3_07	22.00	26.28	+ 19.5	22.00	32.12	+ 46.0
MSD5_02	25.14	16.14	- 35.8	25.14	19.69	- 21.7
MSD5_03	23.62	15.55	- 34.2	23.62	19.09	- 19.2
MSD5_05	19.68	15.55	- 21.0	19.68	19.00	- 3.5
MSD5_07	27.32	22.24	- 18.6	27.32	27.17	- 0.5
MSD5_08	26.54	21.65	- 18.4	26.54	26.57	+ 0.1
MSD5_09	23.00	21.65	- 5.9	23.00	26.57	+ 15.5
MSD5_11	30.17	29.33	- 2.8	30.17	35.83	+ 18.8
MSD5_12	28.61	28.94	+ 1.2	28.61	35.43	+ 23.8
MSD5_13	25.92	28.94	- 11.7	25.92	35.43	+ 36.7

* Used Irwin plastic zone equation $R_p = \frac{1}{\pi}\left(\frac{K}{\sigma_y}\right)^2 \quad \sigma_{coll} = \frac{\sigma_y + \sigma_{ult}}{2}$

When the collapse stress was used, the over prediction for MSD2 and MSD3 increased. The predictions for MSD5 specimens with 7.6 and 12.7 *mm* ligament correlated well with experimental results. However, it over predicted the linkup stress for the 20.3 *mm* ligament by as much as 35%.

The plastic zone linkup criterion was very inconsistent. It may work well for some cases and poorly for other. The ligament length was the dominant variable for the linkup stress. The influence of MSD crack length was secondary.

8 Conclusions

A numerical study of the T_ε^* integral and the CTOA criteria and their use in simulating crack link up and residual strength of test specimens containing MSD have been presented. The study included five different crack configurations, ranging from one to five cracks, to study the T_ε^* integral and CTOA in a single crack environment as well as in a multiple cracks environment with crack interaction.

The T_ε^* integral criterion simulated crack growth and predicted crack linkup and residual strength of panels containing various crack configurations. Instability was assumed to occur when T_ε^* remains greater than $T_{\varepsilon R}^*$ without additional applied displacement or load. The predicted crack linkup and residual strengths correlated very well with the test data. On the average, the predicted maximum loads were within 3% of the test results.

The residual strength predictions using the CTOA criterion were within 5% to 10% of the test results. Where fracture occurs after 1 – 2 *mm* of crack extension, however, the CTOA criterion may not be very reliable.

Predictions using the plastic zone linkup criterion, where the plastic zone equation was derived for a crack in an infinite domain and modified with geometric factors, are inconsistent. The criterion worked well for some cases but poorly for others.

Acknowledgement: This work was conducted under the auspices of the Federal Aviation Administration Grant 91-G-0005 and the U.S. Department of Energy Grant 03-97ER14770.

References

Atluri, S. N.; Nishioka, T.; Nakagaki, M. (1984): Incremental path-independent integrals in inelastic and dynamic fracture mechanics. *Engineering Fracture Mechanics*, vol. 20, no. 2, pp. 209–244.

Brust, F. W.; Nishioka, T.; Atluri, S. N.; Nakagaki, M. (1985): Further studies on elastic-plastic stable fracture utilizing T^* integral. *Engineering Fracture Mechanics*, vol. 22, no. 6, pp. 1079–1103.

Dawicke, D. S.; Newman, J. C. J.; Bigelow, C. A. (1995): Prediction of stable tearing and fracture of 2024-T39 aluminum alloy plate using a CTOA criterion. *NASA Technical Memorandum 109183*.

deWit, R.; Fields, R. J.; Mordfin, L.; Low, S. R.; Harne, D. (1994): Fracture behavior of large-scale thin-sheet aluminum alloy. In *FAA/NASA International Symposium on Advanced Structural Integrity Methods for Airframe Durability and Damage Tolerance*, pp. 963–983. NASA CP 3274.

Gruber, M. L.; Wilkins, K. E.; Worden, R. E. (1996): Investigation of fuselage structure subject to widespread fatigue damage. In *FAA-NASA Symposium for Continued Airworthiness of Aircraft Structure*.

Ma, L. (1999): *Crack Link Up and Residual Strength of Aircraft Structure Containing Multiple Site Damage*. PhD Thesis submitted to the University of Washington.

Nathan, A.; Brot, A. (1991): An analytical approach to multi-site damage. In *Structural Integrity of Aging Airplanes*, pp. 469–492.

Nathan, A.; Brot, A. (1995): Taking multi-site damage past the linear elastic regime (but staying within the engineer's domain). In *ICAF 95: Estimation, Enhancement and Control of Aircraft Fatigue Performance*, pp. 801–814.

Newman, J. C.; Dawicke, D. S.; Bigelow, C. A. (1992): Finite-element analysis and fracture simulation in thin sheet aluminum alloy. In *Durability of Metal Aircraft Structures*, pp. 167–186.

Nikishkov, G. P.; Atluri, S. N. (1987): An equivalent domain integral method for computing crack-tip integral parameter in non-elastic, thermo-mechanical fracture. *Engineering Fracture Mechanics*, vol. 256, no. 6, pp. 851–867.

Nishimura, T. (1999): Strip yield analysis on coalescence of plastic zones for multiple cracks in a riveted stiffened sheet. *Journal of Engineering Materials and Technology, ASME*, vol. 121, pp. 352–359.

Okada, H.; Atluri, S. N. (1999): Further studies on the characteristics of the T_ε^* integral: Plane stress stable crack propagation in ductile materials. *Computational Mechanics*, vol. 23, pp. 339–352.

Okada, H.; Atluri, S. N.; Omori, Y.; Kobayashi, A. S. (1999): Direct evaluation of T_ε^* integral from experimentally measured near tip displacement field. *International Journal of Plasticity*, vol. 15, no. 9, pp. 869–899.

Omori, Y.; Kobayashi, A. S.; Okada, H.; Atluri, S. N.; Tan, P. (1998): T_ε^* as a crack growth criterion. *Mechanics and Materials*, vol. 28, pp. 147–154.

Pyo, C. R.; Okada, H.; Atluri, S. N. (1995): An elastic plastic finite element alternating method for analyzing wide spread fatigue damage in aircraft structure. *Computaional Mechanics*, vol. 16, pp. 62–68.

Schijve, J. (1995): Multiple-site damage in aircraft fuselage structure. *Fatigue and Fracture of Engineering Materials and Structures*, vol. 18, no. 3, pp. 329–344.

Stonesifer, R. C.; Atluri, S. N. (1982): On a study of the (T_ε^*) and C^* integrals for fracture analsyis under non-steady creep. *Engineering Fracture Mechanics*, vol. 16, pp. 769–782.

Swift, T. (1985): The influence of slow stable crack growth and net section yielding on the residual strength of stiffened structure. In *The 13th International Committee on Aeronautical Fatigue*, Pisa, Italy, May 22-24.

Swift, T. (1992): Unarrested fast fracture. In Atluri, S. N.; Harris, C. E.; Hoggard, A.; Miller, N.; Sampath, S. G.(Eds): *Durability of Metal Aircraft Structures*, pp. 419–442.

Swift, T. (1994): Widespread fatigue damage monitoring – issues and concerns. *FAA/NASA International Symposium in Advanced Structural Integrity Methods for Airframe Durability and Damage Tolerance*, pp. 829–870.